LiClO$_4$ Doped Cellulose Acetate as Biodegradable Polymer Electrolyte for Supercapacitors

M. Selvakumar, D. Krishna Bhat

Department of Chemistry, National Institute of Technology Karnataka Surathkal, Srinivasnagar 575025, India

ABSTRACT: The possibility of producing a biodegradable polymer electrolyte based on cellulose acetate (CA) with varied concentration of LiClO$_4$ for use in supercapacitors has been investigated. The successful doping of the CA films has been analyzed by FTIR and DSC measurements of the LiClO$_4$ doped CA films. The ionic conductivity of the films increased with increase in salt content and the maximum ionic conductivity obtained for the solid polymer electrolyte at room temperature was 4.9×10^{-3} Ω^{-1} for CA with 16% LiClO$_4$. The biodegradation of the solid polymer electrolyte films have been tested by soil burial, degradation in activated sludge, and degradation in buffer medium methods. The extent of biodegradation in the films has been measured by AC Impedance spectroscopy and weight loss calculations. The study indicated sufficient biodegradability of the materials. A p/p polypyrrole supercapacitor has been fabricated and its electrochemical characteristics and performance have been studied. The supercapacitor showed a fairly good specific capacitance of 90 F g^{-1} and a time constant of 1 s. © 2008 Wiley Periodicals, Inc. J Appl Polym Sci 110: 594–602, 2008

Key words: solid polymer electrolyte; biodegradation; lithium perchlorate; cellulose acetate; supercapacitor

INTRODUCTION

Electrochemical capacitors (ECs) often called as supercapacitors are currently widely investigated because of their interesting characteristics in terms of power and energy densities.[1] ECs are electrical devices with highly reversible charge storage and delivery capabilities. ECs have properties complementary to secondary batteries. They find usage in hybrid power systems for electric vehicles, starting assist for diesel locomotives, military, and medical applications. ECs employ both aqueous and nonaqueous electrolytes in either liquid or solid state. Solid electrolytes provide the advantages of compactness and reliability without leakage of liquid components. Depending on the charge-storage mechanism, an EC is classified as an electrical double layer capacitor (EDLC) or a pseudocapacitor. Double-layer capacitors have several advantages over secondary batteries, such as faster charge-discharge, longer cycle-life ($>10^5$ cycles), and higher power density. Pseudocapacitors are also called redox capacitors because of the involvement of redox reactions in the charge-storage and delivery processes. Energy storage mechanisms in pseudocapacitors involve fast faradic reactions such as under potential deposition, intercalation, or redox process occurring at or near a solid electrode surface at an appropriate potential. Redox processes often occur in conducting polymers and metal oxides making them attractive materials for pseudocapacitors.[1–3] Polymer electrolytes, such as polyethylene oxide-salt complexes,[4–7] which are prepared by doping of ionic salt to polymers are the most common solid electrolytes employed in electrochemical devices. Solid polymer electrolytes have ionic conductivity between 10^{-8} and 10^{-7} S cm^{-1}, which are too low to be of use in practical devices. Efforts have therefore been expended to enhance the ionic conductivity of polymer electrolytes by different techniques.[4] However, little attention has been paid to the polymer electrolytes that are hazardous to the environment, when used in large amounts. Intensive work is being done on developing various materials and the use of environmentally conscious materials or ecomaterials during manufacturing, which can help to reduce the environmental impact of many products throughout all phases of the product life cycle.[8–10] The use of biodegradable polymers has contributed to a reduction in environmental problems. As a result, there has been a trend toward the production of degradable natural and synthetic polymers and natural/synthetic polymer blends.[11,12] Among biodegradable synthetic polymers, cellulose acetate (CA) is one of the most attractive polymers because of its availability, degradation in the environment, and good mechanical properties. Further, there are only very few reports on biodegradable

polymer electrolytes for use in electronic devices.[10,13] For example Lopes et al.[14] have studied starch doped with lithium perchlorate in the presence of plasticizer as a polymer electrolyte. The observed conductivity in this case ranged from 3×10^{-4} to 2×10^{-3} S cm^{-1}. The conductivity of the polyelctrolyte formed by polyvinylalcohol and polyacrylic acid blends[15] in presence of different dopants varied in the range 10^{-3} to 10^{-1} S cm^{-1}. The polyelectrolyte reported by Viera et al.,[16] based on gelatin in presence of plasticizers showed conductivity in the range, 4.5×10^{-5} to 3.6×10^{-4}. In view of the aforesaid discussion, we have chosen LiClO$_4$ doped CA as a biodegradable solid-polymer electrolyte for use in supercapacitors. These CA films showed good water retention capacity and ionic conductivity of the polymer electrolytes increased with increase in dopant concentration.

In this article, as a part of our ongoing research program on biodegradable polymers[11] and conducting polymer devices,[17,18] we provide the first report of an ionic system based on a biodegradable polymer, CA, with different concentrations of LiClO$_4$. The purpose of this work was to apply a biodegradable solid polymer electrolyte to a supercapacitor with the goal of preventing or reducing dendrite formation, leakage of electrolyte, and more importantly for low environmental impact when the device is discarded. The biodegradation behavior of the solid polymer electrolyte and electrochemical properties of a p/p polypyrrole(PPy) supercapacitor fabricated using this solid-polymer electrolyte have been evaluated and presented in this article.

EXPERIMENTAL

Materials

All the chemicals used were of analytical reagent grade. CA (number-average molecular weight: 70,000), p-toluenesulfonic acid, KH$_2$PO$_4$, and Na$_2$HPO$_4$ were all obtained from CDH, India; LiClO$_4$ from Loba Chemie, India; tetrahydrofuran (THF) from Nice, India and used after distillation. Pyrrole (Acros Organics, Beel, Belgium) was used after vacuum distillation. Double distilled water was used for the preparation of aqueous solutions.

Solid biodegradable polymer electrolyte preparation

The biodegradable electrolyte was prepared by dissolving CA and LiClO$_4$ in THF. The solvent was evaporated and dried at high vacuum for 48 h. The salt concentration was 2, 5, 10, 12, and 16 wt % of LiClO$_4$. Double distilled water was used wherever needed.

Spectral and thermal studies

The FTIR measurements of the polymer electrolyte films were carried out on NICOLET AVATAR 330 FTIR Spectrometer and DSC measurements to determine the T_g of the LiClO$_4$ doped CA samples were done on a DSC SP Model instrument from Rheometric Scientific, Ashtead, UK. Measurements were performed over a temperature range of 25–300°C at a heating rate of 10°C min^{-1} under the nitrogen atmosphere.

Biodegradation tests[12,19–21]

Soil burial degradation

The soil used was obtained from N.I.T.K. garden. The soil was slightly acidic with a pH value of 6.7. The characteristics of the soil used were as follows: class, Ultisol (loamy type); electrical conductivity, 0.08 dS m^{-1}; organic carbon, 33 g kg^{-1}; CEC, 16.2 cmol kg^{-1}; average nitrogen, 151.4 mg kg^{-1}; average phosphorus, 5 mg kg^{-1}; Ex. K: 0.15 cmol kg^{-1}; Ex. Ca: 4.6 cmol kg^{-1}; Ex. Mg: 1.4 cmol kg^{-1}; Ex. Na: 0.2 cmol kg^{-1}. The preweighed polyblend films were buried in soil in desiccators. The soil was maintained at $\sim$ 20% moisture weight. The desiccators were kept at room temperature and the average temperature during the study period was 30°C. The films were taken out, washed with water, dried, weighed, and resistance of the solid-polymer electrolyte was measured accurately using AC impedance spectroscopy to know the degradation in the intervals of 15, 45, and 60 days.

Degradation in activated sludge

Activated sludge in the form of slurry was obtained from nearby BASF plant. The sludge had the following characteristics: mixed liquor suspended solids, 4000 mg L^{-1}; liquid content, 45%; pH, 8.1; COD without biomass, 235 ppm; color, 348 Hazen units; C, 52%; H, 07%; O, 22%; N, 16%; P, 1.2%; S, 1.7%. Fixed volumes of activated sludge solutions were taken in glass jars. The preweighed blend films were kept immersed in the solution and the solution was aerated intermittently by air bubbling using a pump, to keep aerobic condition. The films were removed from the sludge solution after 5, 10, 15 days, washed well with double distilled water, and dried in a hot air oven at 75°C to perfect dryness, weighed and then resistance of the solid-polymer electrolyte was measured accurately using AC impedance spectroscopy to know the degradation in the intervals of 5, 10, and 15 days.

Hydrolytic degradation in buffer solutions

The weighed blend films were kept immersed in phosphate buffer solution of pH = 7.5 in a glass jar
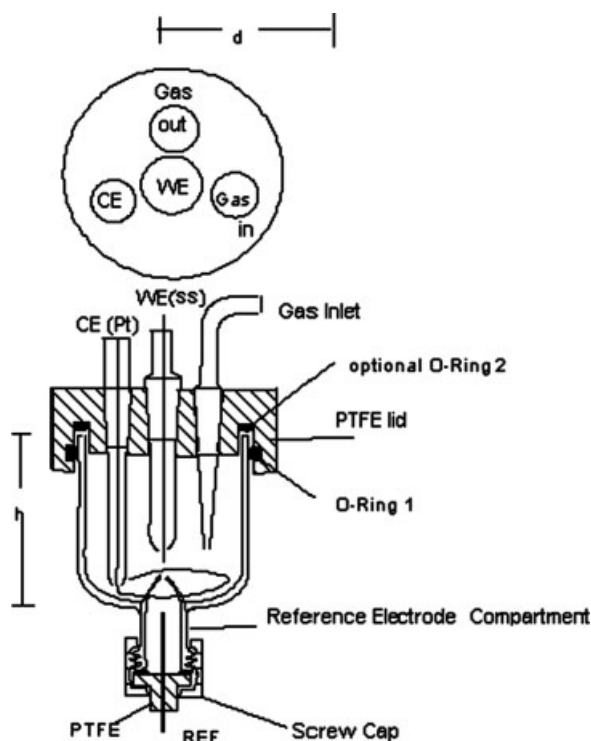
Figure 1 Schematic diagram of the cell used for the electrochemical studies.

at room temperature (30°C). The buffer solutions were prepared by making use of KH_2PO_4 and Na_2HPO_4 solutions. After designated time intervals (5, 10, 15 days) the films were removed; well washed with water, dried, weighed and then resistance of the solid-polymer electrolyte films was measured accurately using AC impedance spectroscopy to know the degradation in the intervals of 5, 10, and 15 days.

Electrochemical characterization

Polypyrrole was galvanostatically deposited onto the stain less steel (SS) electrode with a constant current density of 0.3 mA cm^{-2} for 500 s. The electrolyte was prepared by mixing the desired amount of pyrrole monomer and *p*-toluenesulphonic acid in a suitable concentration of aqueous acidic solution. A single compartment cell was used for characterizing the polymer deposited onto the SS substrate by cyclic voltammetry (CV). SS electrode (3 cm × 2 cm) was used as the working electrode, platinum foil (5 cm^2) was used as counter electrode and saturated calomel electrode (SCE) was used as the reference electrode (Fig. 1).

The capacitor cells were constructed with a $LiClO_4$ doped CA electrolyte impregnated separator sandwiched between two symmetrical PPy deposited electrodes (Fig. 2). Electrochemical characterization of the PPy deposited electrode was carried out by

CV, electrochemical impedance spectroscopy (EIS), and galvanostatic charge-discharge studies. All the electrochemical studies were carried out using an AUTOLAB Electrochemical System (Eco Chemie BV, The Netherlands).

The bulk ionic conductivities (σ) of the $LiClO_4$ doped CA were determined from the impedance spectra in the frequency range between 100 mHz and 10 kHz with a perturbation of 5 mV rms, The EIS studies of the supercapacitor was performed in the frequency range between 10 mHz and 1 MHz with a perturbation of 5 mV rms. The charge-discharge behavior of the fabricated supercapacitor was analyzed by galvanostatic method.

RESULTS AND DISCUSSION

FTIR studies

FTIR is an appropriate method[22] for monitoring the coordination or complexation of Li -ion with the polymer, CA. Certain bands resulting from specific vibrations of each of the potentially coordinating species have been observed to split or shift to different frequencies on cation coordination. FTIR spectra of pure CA and $LiClO_4$ doped CA films are shown in Figures 3 and 4. The intermolecular hydrogen bonded O—H stretching frequency of molecules are generally observed[23] in the region, 3400–3600 cm^{-1}. This frequency for pure CA, in our case is observed at 3679 cm^{-1}. This is due to the presence of moisture in the sample, which was not completely removed. The same frequency is shifted to 3676 cm^{-1} in Li-salt complexed CA. The symmetric and anti symmetric aliphatic C—H stretching together with
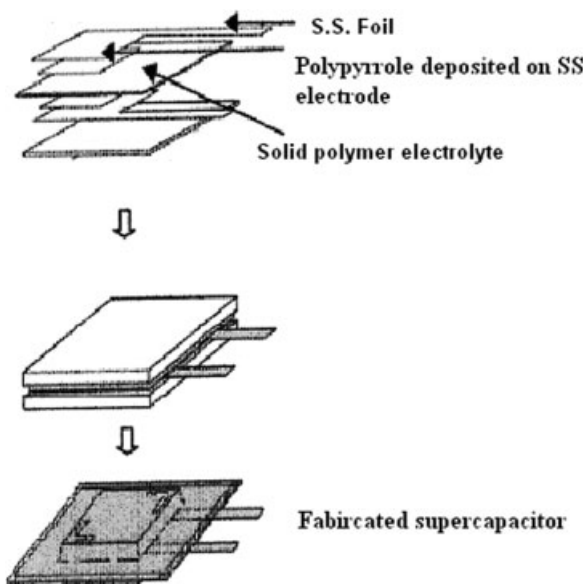

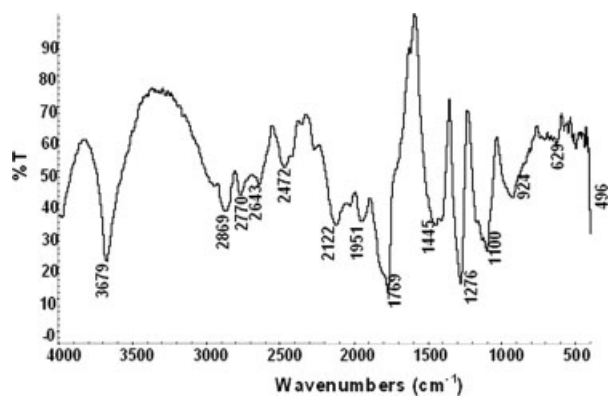**Figure 2** Scheme for the assembling of the supercapacitor.

Figure 3 FTIR spectra of CA.

Figure 5 DSC scan images of polyelectrolyte films at varying Li salt contents: (a) 0%, (b) 2%, (c) 5%, (d) 10%, (e) 12%, (f) 16%.

contributions from H-bonded hydroxyl stretching occurs between 3100 and 2400 cm^{-1}. The major frequency for the same is observed at 2869 cm^{-1}, for pure CA, has been shifted to 2874 cm^{-1} in the salt complex. A group of stretching vibrations in pure CA in this region is merged to almost a single frequency at 2874 cm^{-1} in the salt complex. The carbonyl stretching vibration found at 1769 cm^{-1} for pure CA has been shifted to 1768 cm^{-1} for the complex. The CH$_2$ deformation vibration or scissoring frequency occurred at 1445 cm^{-1} with strong intensity for pure CA is observed at 1450 cm^{-1} for salt doped CA. A sharp strong peak due to C—O—C anti symmetric stretching vibrations of ester group of pure CA is observed at 1276 cm^{-1}. This frequency is shifted to 1280 cm^{-1} in the LiClO$_4$-CA complex. The C—OH stretching vibration of pure CA observed at 1100 cm^{-1}, has been shifted to 1105 cm^{-1} in the case of its salt complex. A medium peak at 924 cm^{-1} in pure CA may be due to the combined contributions from C—O stretching and CH$_2$ rocking vibrations. This peak is shifted to 917 cm^{-1} in the salt complex. The symmetric vibration of ClO$_4^-$ is generally observed at 940 cm^{-1}. As in our case, this
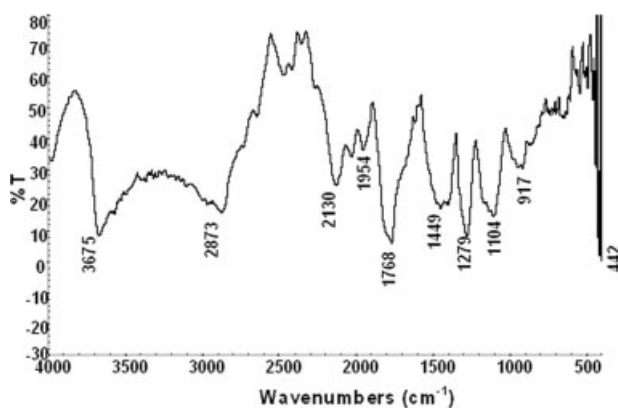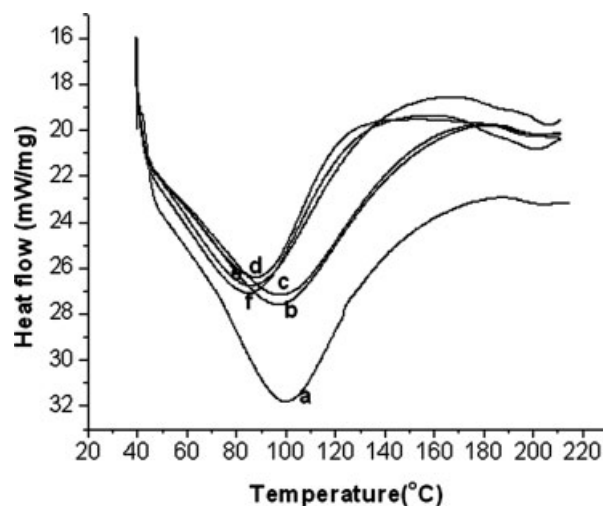
frequency region overlaps with that of C—O stretching of CA and a reduced frequency of the same is observed at 917 cm^{-1} in the salt complex. The reduction in the frequency must be due to the complexation effect. Further, it may also be noted that the intensity of all the peaks in the FTIR spectrum of salt complex is less and broader when compared with that of the pure CA spectrum. Such effects are generally brought about by complexation of the substrate molecule (CA) by the dopant (LiClO$_4$) due to intermolecular interactions.[24,25] Hence the formation of LiClO$_4$-CA complex or successful doping of CA is confirmed.

DSC studies

Figure 5 presents the T_g of CA films with varying amounts of doped LiClO$_4$. The T_g of the films decreased gradually from 105°C in the case of pure CA to 83°C for CA with 16% of doped salt. This is due to the fact that the added salt disrupts the intermolecular interactions within the host molecule to set up new interactions, which in turn can increase the entropy of mixing. This increase in the entropy of mixing increases the segmental movements leading to reduction in the crystallinity and enhancement in the flexibility of the molecular system. All these processes finally result in the decrease of the T_g of the sample. These observations are also in conformity with that reported.[15,26,27]

Ionic conductivity studies

The bulk ionic conductivities (σ) of the solid polymer electrolytes were (Table I) determined from the complex impedance spectra using the equation, $\sigma = L/RA$, where L, R, and A are, respectively, the

Figure 4 FTIR spectra of LiClO$_4$ doped CA.

TABLE I
Variation of Conductivity of Polyelectrolyte Films Under
Different Test Conditions and Salt Concentrations

	Conductivity (10^{-5} S cm^{-1})					
A	B	C	D	E	F	G
0	0.11	0.21	0.20	0.48	0.20	0.40
2	1.00	0.20	0.68	0.47	0.78	4.70
5	21.2	4.13	9.73	3.26	11.7	5.25
10	74.3	9.57	36.4	6.12	42.6	9.76
12	340.4	57.5	82.6	7.29	98.7	15.1
16	490.7	72.3	102.5	9.27	118.4	21.6

A, % of LiClO$_4$ in cellulose acetate; B, Before degradation; C, After 60 days of soil-burial degradation; D, After 5 days in Activated sludge; E, After 15 days in Activated sludge; F, After 5 days of buffer degradation; G, After 15 days of buffer degradation.

thickness, bulk resistance, and area of the solid polymer electrolyte. The bulk resistance was calculated from the high frequency intercept on the real impedance axis of the Nyquist plot.[15] The effect of amorphicity on the ionic conductivity of the nonaqueous polymer electrolytes with metal salts has been extensively studied in the literature.[15,28–30] Decrease in T_g accompanied by an increase in amorphicity has been reported to increase the segmental motion in polymer electrolytes that in turn enhances the ionic conductivity. Figure 6 presents the ionic conductivity data for the solid polymer electrolytes. The ionic conductivity of the samples varies in the range, 1.1×10^{-6} S cm^{-1} for pure CA to 4.9×10^{-3} S cm^{-1} in the case of CA with 16% of Li salt content. The ionic conductivities of the samples increased with increase in Li salt content. This increase in ionic conductivity was steep at higher Li salt content. The dynamic percolation model,[28] developed by Druger, Nitzan, and Ratner for ion conduction in polymer electrolytes envisages ionic motion in terms of jumps between energetically equivalent neighboring positions. As shown in Figure 7, a cation (M$^+$) being a Lewis acid, links with Lewis bases, B such as oxygen atoms associated with a polymer chain. The jump of a cation from one site to an energetically equivalent neighboring site takes place by a slow change in the local environment as a single M$^+$-B linkage evolves with time. As the polymer gradually changes its conformation due to segmental motion, an accompanying translation of the cation to the neighboring site follows. The increased polymer segmental motion in CA-Li salt complex, resulting from the increased amorphicity or disorder due to increase in the Li salt content in the polymer electrolyte complex, brought about an increase in the entropy in the system and this causes the increase in the ionic conductivity of the polymer electrolyte.[15,28–30]

Biodegradation studies

The biodegradation behavior of the solid polymer electrolyte films have been studied by conductivity analysis through AC impedance spectroscopy and also by weight loss method under different test conditions. AC impedance spectroscopy is a nondestructive and informative technique commonly used in corrosion science and coating characterization for determining delamination and failure in corrosion coating resistance. Changes in the impedance signal can be correlated to the performance of the materials. The AC impedance technique can be efficiently used for the evaluation of polymer degradation and the use of this method has also been well illustrated in the literature.[31–35] The variation of conductivity of the samples under different test conditions and with time has been presented in Table I. The ionic conductivity of pure CA film slightly increased during all degradation conditions with time. The conductivity varied from 1.1 μS cm^{-1} (before degradation test) to a maximum of 4.8 μS cm^{-1} in the case of pure CA under biodegradation in activated sludge for 15 days. The conductivity values for other degradation test conditions were in between these values. This may be due to the absorption of water followed by the swelling of the polymer electrolyte film which can slowly start the fragmentation of the polymer matrix leading to the increased flexibility of the polymer chains and hence the slightly increased conductivity. The conductivity of Li salt doped CA films decreased with time under different degradation tests. As already discussed above, the presence of added Li salt increases the flexibility of the polymer electrolyte films. This can facilitate the absorption of moisture and swelling and hence triggers the hydrolytic degradation and even can attract attack from microorganisms. During this biodegradation process,
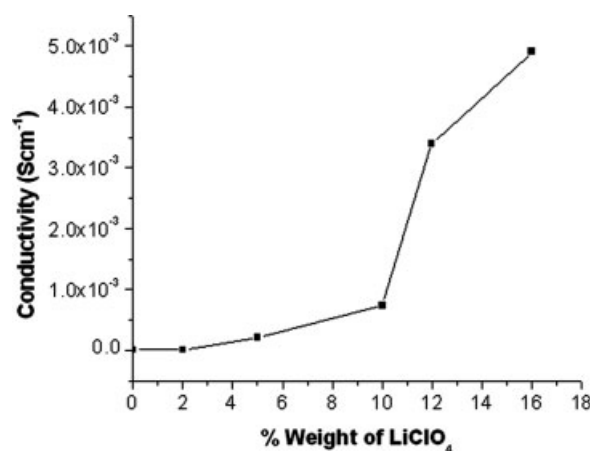

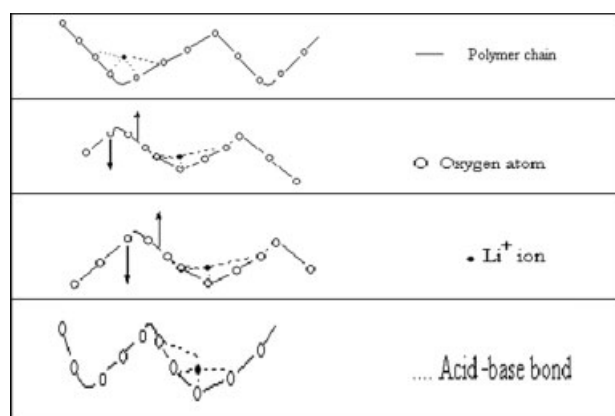**Figure 6** Ionic conductivity of polyelectrolyte films as a function of Li salt content.

Figure 7 Segmental motion mechanism of ionic conduction in the polyelectrolytes.

Figure 9 Degradation of LiClO$_4$ doped CA films in activated sludge.

along with the fragmented polymer molecules, Li salt also gets lost in the degrading environment. As the conductivity depends on the salt content, the ionic conductivity of the biodegraded samples decreased with time under biodegradation study.

Soil burial degradation

A short-term study for a period of 60 days has been conducted on the soil degradation behavior of CA-Li salt complex films. Although long-term studies are more useful in characterizing the soil degradation of matrices (e.g., for a year or two), the short-term study does give an insight into the blend behavior and can be used for a rapid evaluation of biodegradability of polymers.[11] In this study, the polyelectrolyte films showed degradation of the order of about 0.35–3.4% (Fig. 8). The film with higher Li salt content showed maximum degradation. The polymers exposed to soil might have initially undergone biodegradation, where microorganisms consume the natural cellulose component. Consequently, the oxy-
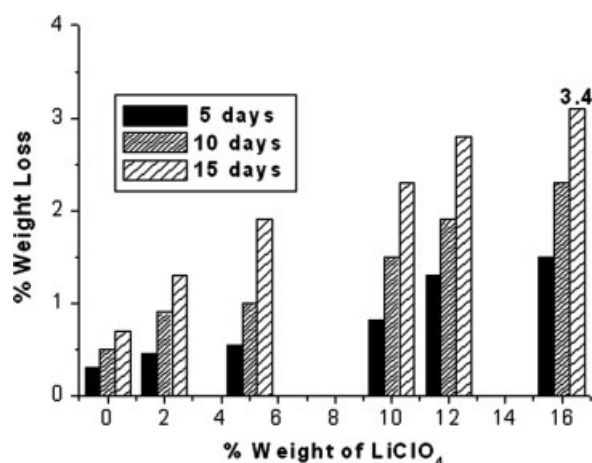
gen can attack the newly generated surface with the formation of peroxides, hydro peroxides, oxides, etc., which promote the scission of polymeric chains into small fragments more susceptible to the attack of microorganisms.[11,12,20,21,36] Soil bacteria and fungi might be responsible for the degradation.[20]

Degradation in activated sludge

Degradation of the CA-Li salt complex films in the activated sludge was monitored for 15 days. The polymers showed sufficient degradation and the extent of degradation was 0.5–5%. The CA-Li salt complex film with higher Li salt content degraded to the maximum extent (Fig. 9). Hydrolytic degradation as well as degradation by microorganisms might be responsible for the decay. The degradation of the films was higher in activated sludge compared with other tests. This may be due to the fact that in this test there is a combined effect of both hydrolysis and microbial attack.[11,12,19–21]

Hydrolytic degradation in buffer solutions

CA-Li salt complex films showed considerable degradation in phosphate buffer solutions. The degradation was found to be in the range of 0.45–4% for various compositions (Fig. 10). Even in this study, biodegradation was maximum in the case of film with higher salt content. As the constituents of the CA-Li salt complex films were ester and an inorganic salt, hydrolysis could have been the major mode of degradation. The hydrolysis products would be, organic acids, methanol, cellulose, etc., are compounds which are easily attacked by microorganisms to undergo further degradation. Hence hydrolysis followed by microbial degradation may be the path of degradation in buffer solutions.[12,20]
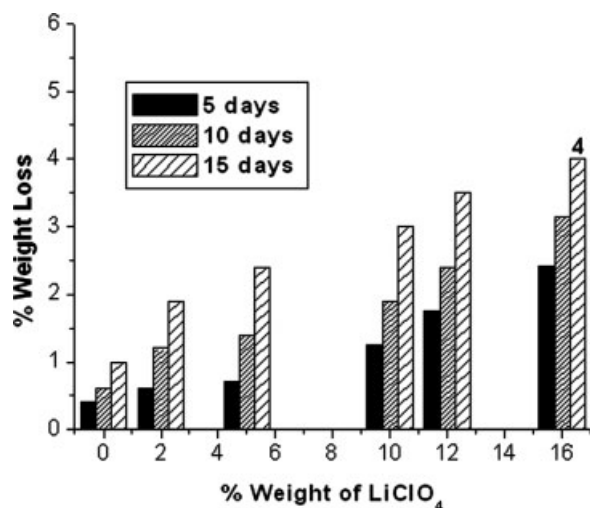

Figure 8 Degradation of LiClO$_4$ doped CA films in soil.

Figure 10 Degradation of $LiClO_4$ doped CA films in buffer solution.

In all the above tests, the maximum extent of biodegradation observed in the case of pure CA film was only up to 1.2% (activated sludge test), whereas the same in the case of CA-Li salt complex films was much higher. This distinct difference clearly indicates the influence of Li salt complexation in promoting the biodegradation of polyelectrolyte material. This behavior is also in conformity with that reported.[8–10]

Electrochemical studies

Cyclic voltammograms (CV) for polypyrrole deposited on stainless steel (SS) electrode at various sweep rates are shown in Figure 11. The single electrode responses clearly show the capacitive characteristics as well as the corresponding redox features of polypyrrole under doping and dedoping. The CV for the supercapacitor cell fabricated using the biodegradable electrolyte is shown in Figure 12. The CV exhibits the typical features of redox capacitive features
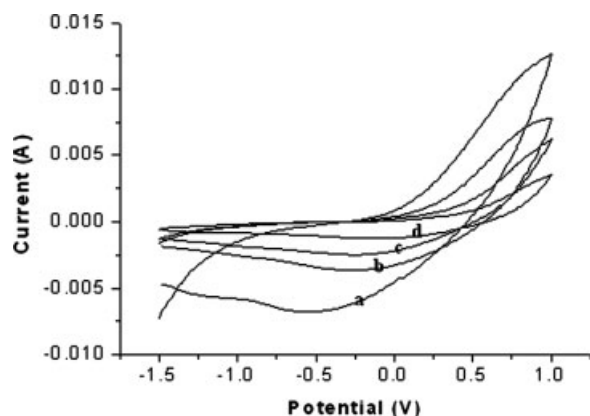

Figure 11 CVs of polypyrrole deposited on SS electrodes at (a) 50 mV s^{-1}, (b) 25 mV s^{-1}, (c) 20 mV s^{-1}, (d) 10 mV s^{-1}.
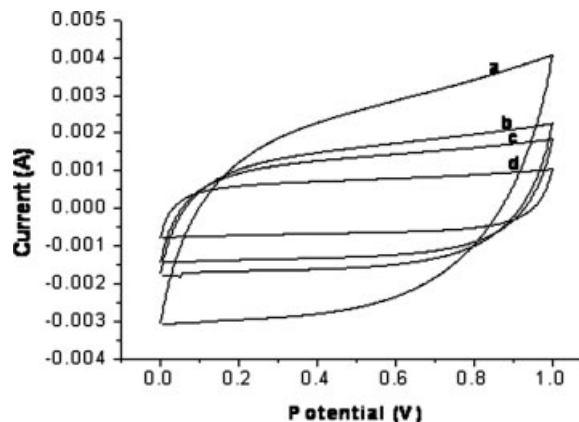
Figure 12 CVs of the fabricated p/p polypyrrole symmetric supercapacitor using biodegradable polymer electrolyte at scan rates; (a) 50 mV s^{-1}, (b) 25 mV s^{-1}, (c) 20 mV s^{-1}, (d) 10 mV s^{-1}.

and the observed patterns are in conformity with that reported.[1–3,13,17,18,37]

The capacitance values for the symmetric capacitor (Table II) have been calculated[38] from the cyclic voltammograms using the equation: $C = i/s$, where "s" is the potential sweep rate and "i" is the average current. Specific capacitance of 150 F g^{-1} was obtained for the single electrode at the sweep rate of 10 mV s^{-1}. The same for the fabricated biodegradable solid polymer electrolyte based supercapacitor was 90 F g^{-1}. This value is also comparable to that reported.[2,17,18] The reduction in the capacitance in the case of supercapacitor is quite normal because in the supercapacitor fabrication, the two polypyrrole electrodes constitute the electrochemical configuration of a parallel plate condenser connected in series. The AC impedance response of capacitor is shown in Figure 13. A semicircle is obtained at high frequency in the range 100 kHz to 10 Hz and almost a straight line in the low frequency region. The capacitance values increase at low frequencies. This is because of the decrease in the bulk resistance of the capacitor caused due to the motion of large number of ions at low frequencies. The semicircle results from the parallel combination of resistance and capacitance and the linear region is due to Warburg

TABLE II
Specific Capacitance Values of the PPy Single Electrode and Super Capacitor Based on the Solid Polymer Electrolyte

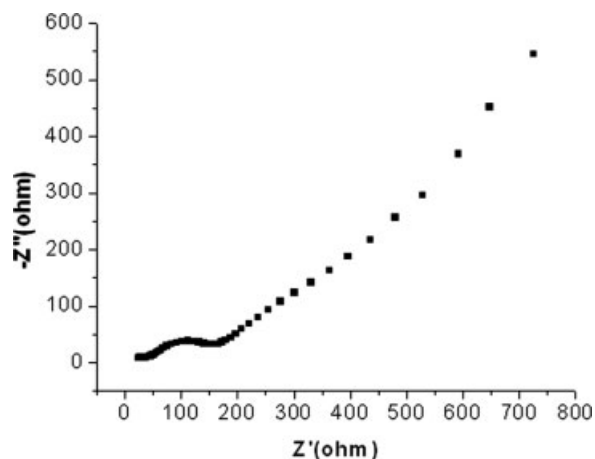| Scan rate (mV s^{-1})	Specific capacitance of single electrode (F g^{-1})	Specific capacitance of symmetric supercapacitor (F g^{-1})
50	75	40
25	110	50
20	125	65
10	150	90

Figure 13 AC impedance spectra of the fabricated p/p polypyrrole symmetric supercapacitor using biodegradable polymer electrolyte.

Figure 15 Galvanostatic charge-discharge plots of the biodegradable polymer electrolyte p/p polypyrrole symmetrical supercapactior for the first 10 cycles.

impedance. In the low frequency region, the AC impedance plot leans more towards imaginary axis. This is an indication of good capacitive behavior.[37] These electrochemical impedance data have been analyzed[37] by plotting the normalized imaginary part /Q///S/ and real part /P///S/ of the complex power (S) versus frequency and are shown in Figure 14, The relaxation time constant of the supercapacitor determined from these data was found to be one second.

Figure 15 shows the charge-discharge profile of the super capacitor as measured by galvanostatic method at a constant current density of 2 mA cm^{-2} at different cycles between 0 and 1.0 V, for the first 10 cycles. From the figure, it can be seen that the voltage of the capacitor varies almost linearly with time during both charging and discharging processes for various cycles. It is evident from the figure
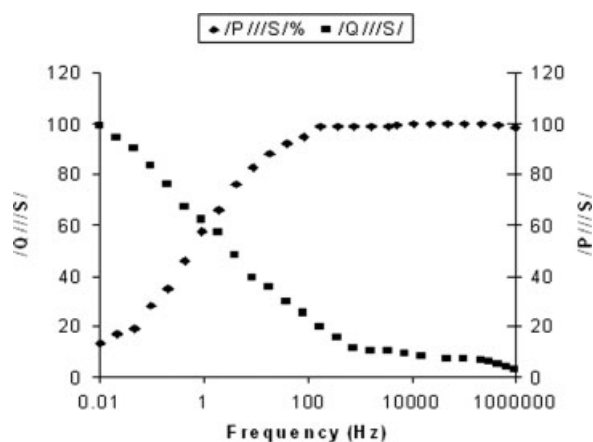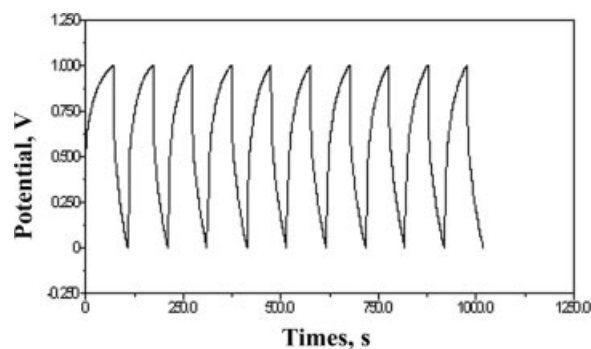
that the charging time and also discharging time remained constant with increasing number of cycles. However, there may be a slightly higher voltage drop and decrease in the charging and discharging time with cyclings as well as with current density beyond 1000 cycles or so due to the degradation possibility of the cell redox activity.[37] The coulombic efficiency of the supercapacitor calculated from charge-discharge cyclings is also high in the range of 98–99%. Figure 16 presents the variation of specific capacitance of the supercapacitor with cyclings. The data reflects that the device exhibited almost constant capacitance during the test. However, at higher cycle numbers the capacitance is expected to decrease slightly due to the decrease of redox activity of the supercapacitor.[15]

CONCLUSIONS

In this study, possibility of producing a biodegradable polymer electrolyte by doping CA polymer

Figure 14 Plots of normalized reactive power /Q///S/% and active power /P///S/% versus frequency (Hz) for the biodegradable polymer electrolyte based p/p polypyrrole symmetrical supercapacitor.
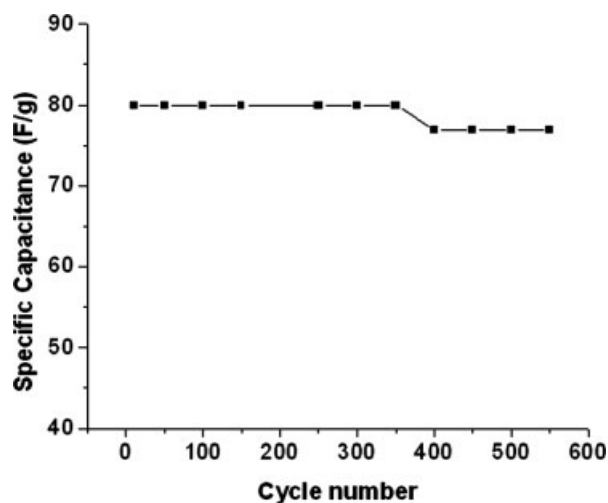

Figure 16 Variation of specific capacitance of the supercapacitor with cycle numbers.

with lithium perchlorate has been investigated. The CA-LiClO$_4$ films prepared were auto-supported, flexible, and apparently homogeneous. The maximum ionic conductivity obtained at room temperature was 4.9×10^{-3} S cm^{-1} for CA with 16% LiClO$_4$. The ionic conductivity in these films has been attributed to the operation of segmental motion type of mechanism. The polyelectrolyte material has been studied for its biodegradation behavior by subjecting the material to different degradation tests based on weight loss method and conductivity measurement by AC impedance spectroscopy. The study revealed that the material has sufficient biodegradability and that the salt complexation increases the biodegradability. A p/p polypyrrole symmetric supercapacitor has been fabricated using this biodegradable material and its performance has been tested. The supercapacitor has also shown good capacitive nature and was stable during cyclings. Hence the study demonstrates the successful preparation of a biodegradable polyelectrolyte for use in supercapacitors.

References

1. Conway, B. E. Electrochemical Supercapacitors: Scientific Fundamentals and Technological applications; Kluwer Academic/Plenum Press: New York, 1999.
2. Mastragostino, M.; Arbizzani, C.; Soavi, F. Solid State Ionics 2002, 148, 493.
3. Conway, B. E. J Electrochem Soc 1991, 138, 1539.
4. MacCallum, J. R.; Vincent, C. A., Eds. Polymer Electrolyte Review, Vol. 1/2; Elsevier: London, 1987–89.
5. Gray, F. M. Solid Polymer Electrolytes—Fundamentals and Technological Applications; VCH: Weinheim, 1991.
6. Scrosati, B. Applications of Electroactive Polymers; Chapman and Hall: London, 1993.
7. Abraham, K. M.; Alamgir, M. J Electrochem Soc 1990, 127, 1657.
8. Rosa, D. S.; Neto, I. C.; Calil, M. R.; Pedroso, A. G.; Fonseca, P. C.; Neves, S. J Appl Polym Sci 2004, 91, 3909.
9. Fonseca, P. C.; Neves, S. J Power Sources 2006, 159, 712.
10. Fonseca, P. C.; Neves, S. J Power Sources 2004, 135, 249.
11. Krishna Bhat, D.; Selvakumar, M. J Polym Environ 2006, 14, 385.
12. Chandra, R.; Rustgi, R. Prog Polym Sci 1998, 23, 1273.
13. Fonseca, P. C.; Rosa, D. S.; Gaboardi, S.; Neves, S. J Power Sources 2006, 155, 381.
14. Lopes, L. V. C.; Dragunski, D. C.; Pawlicka, A.; Donoso, J. P. Electrochimica Acta 2003, 48, 2021.
15. Choudhury, N. A.; Shukla, A. K.; Sampath, S.; Pitchumani, S. J Electrochem Soc 2006, 153, A614.
16. Vieira, D. F.; Avellaneda, C. O.; Pawlicka, A. Electrochimica Acta 2007, 53, 1404.
17. Krishna Bhat, D.; Selvakumar, M. J Mater Sci 2007, 42, 8158.
18. Selva Kumar, M.; Krishna Bhat, D. J Appl Polym Sci 2008, 107, 2165.
19. Zhang, L.; Deng, X.; Zhao, S.; Huang, Z. Polymer 1997, 38, 6001.
20. Okada, M.; Yamada, M.; Yokoe, M.; Aoi, K. J Appl Polym Sci 2001, 81, 2721.
21. Chandra, R.; Rustgi, R. Polym Degrad Stab 1997, 56, 185.
22. He, W.; Zhu, B.; Inoue, Y. Prog Polym Sci 2004, 29, 1021.
23. Lambert, J. B.; Shurvell, H. F.; Lighter, G. A.; Cooks, R. G. Introduction to Organic Spectroscopy; Macmillan: New York, 1992.
24. Rajendran, S.; Sivakumar, M.; Subadevi, R. Solid State Ionics 2004, 167, 335.
25. Stephen, A. M.; Premkumar, T.; Renganathan, N. G.; Pitchumani, S.; Thirunakaran, R.; Muniyandi, N. J Power Sources 2000, 89, 80.
26. Kuo, P. L.; Liang, W. J.; Chen, T. Y. Polymer 2003, 44, 2957.
27. Lai, S. M.; Huang, C. K.; Shen, H. F. J Appl Polym Sci 2005, 97, 257.
28. Ratner, M. A.; Shriver, D. F. Chem Rev 1988, 88, 109.
29. Zheng, J. P.; Cygyan, P. J.; Jow, T. R. J Electrochem Soc 1995, 142, 2699.
30. Zheng, J. P.; Jow, T. R. J Electrochem Soc 1995, 142, L6.
31. Kremer, F.; Schonhals, A. Broadband Dielectric Spectroscopy; New York: Springer, 2003.
32. Amareshwar, P.; Radhakrishnan, M. J Polym Mater 2000, 17, 473.
33. Tchmutin, I.; Ryvkina, N.; Saha, N.; Saha, P. Polym Degrad Stab 2004, 86, 411.
34. Gu, J.-G.; Cheng, S.-P.; Liu, J.; Gu, J.-D. J Polym Environ 2000, 8, 167.
35. Gu, J.-G.; Gu, J.-D. J Polym Environ 2005, 13, 65.
36. Scidenstriker, T.; Fritz, H. G. Polym Degrad Stab 1998, 59, 279.
37. Taberna, P. L.; Simon, P.; Fauvarque, J. F. J Electrochem Soc 2003, 150, A292.
38. Muthulakshmi, B.; Kalpana, D.; Pitchumani, S.; Renganthan, N. G. J Power Sources 2005, 158, 1533.